

# Periodic and quasiperiodic motions of many particles falling in a viscous fluid

M. Gruca<sup>1</sup>, M. Bukowicki<sup>1</sup> and M. L. Ekiel-Jeżewska<sup>1</sup> †,

<sup>1</sup>Institute of Fundamental Technological Research, Polish Academy of Sciences,  
02-106 Warsaw, Pawińskiego 5b, Poland

(Received ?)

Dynamics of regular clusters of many non-touching particles falling under gravity in a viscous fluid at low Reynolds number is analyzed within the point-particle model. Evolution of two families of particle configurations is determined: 2 or 4 regular horizontal polygons (called ‘rings’) centered above or below each other. Two rings fall together and periodically oscillate. Four rings usually separate from each other with chaotic scattering. For hundreds of thousands of initial configurations, a map of the cluster lifetime is evaluated, where the long-lasting systems are centered around periodic solutions for the relative motions. The results illustrate that the existence of periodic solutions is essential for clustering of many sedimenting particles.

## 1. Introduction

From both practical and fundamental points of view, it is important to understand the mechanism of clustering of many particles sedimenting in a viscous fluid at the low-Reynolds-number. The dynamics of benchmark systems of three and four particles falling under gravity in a viscous fluid have been already extensively studied. Several classes of periodic solutions have been found theoretically, e. g. by Hocking (1963), Caffisch *et al.* (1988), Tory *et al.* (1991), Ekiel-Jeżewska, Gubiec & Szymczak (2008), and experimentally, e. g. by Jayaweera *et al.* (1964). The chaotic scattering of three sedimenting particles have been shown by Janosi *et al.* (1997), Ekiel-Jeżewska & Wajnryb (2011), and sensitivity of the cluster lifetime to initial conditions has been related to the existence of periodic solutions, found by Ekiel-Jeżewska (2008).

The question is if a similar relation can be observed for systems of many particles. To answer this question, it is convenient to generalize the results of Ekiel-Jeżewska (2014), who found periodic solutions for a moderate number of particles centered at vertices of two regular horizontal polygons (‘rings’), and long-lasting quasiperiodic relative motions of particles in a perturbed system which consists of 4 rings.

Therefore, in this work we first demonstrate that 2 rings made of a very large number of particles indeed fall oscillating periodically, and next investigate in details the dynamics of 4 rings for a wide range of the initial conditions and different numbers of particles. We evaluate a map of the cluster lifetimes, and search for periodic solutions.

## 2. System and its theoretical description

We investigate dynamics of regular groups of many point-particles settling under identical gravitational forces  $\mathbf{G}$  in a fluid of viscosity  $\eta$  at the low-Reynolds-number. The fluid

† Email address for correspondence: mekiel@ippt.pan.pl

velocity  $\mathbf{v}$  and pressure  $p$  satisfy the Stokes equations, see e.g. Kim & Karrila (2005),

$$\eta \nabla^2 \mathbf{v}(\mathbf{r}) - \nabla p(\mathbf{r}) = - \sum_{i=1}^M \mathbf{G} \delta(\mathbf{r} - \tilde{\mathbf{r}}_i), \quad \nabla \cdot \mathbf{v}(\mathbf{r}) = 0. \quad (2.1)$$

where  $M$  is the number of particles,  $\tilde{\mathbf{r}}_i$  denotes the position of the particle with label  $i$ , and the  $z$ -axis is chosen along gravity, with  $\mathbf{G} = -G\hat{\mathbf{z}}$  where  $G > 0$  and  $\hat{\mathbf{z}}$  is the unit vector along the  $z$ -axis.

From now on, we use dimensionless variables, based on a size of the group  $d$  as the length unit, and  $G/(8\pi\eta d)$  as the velocity unit. Therefore,  $8\pi\eta d^2/G$  is the time unit. It is convenient to follow Mylyk *et al.* (2011) and choose a frame of reference moving with the Stokes velocity of the isolated particle.

With this choice, the equations of motion of the particles are given by

$$\frac{d\mathbf{r}_i}{dt} = - \sum_{j \neq i}^M \mathbf{T}(\mathbf{r}_{ij}) \cdot \hat{\mathbf{z}} \quad (2.2)$$

where  $\mathbf{r}_i = \tilde{\mathbf{r}}_i/d$  is the dimensionless position of a particle  $i$ ,  $\mathbf{r}_{ij} = \mathbf{r}_i - \mathbf{r}_j$ , and  $\mathbf{T}(\mathbf{r}) = (\mathbf{I} + \mathbf{r} \otimes \mathbf{r}/|\mathbf{r}|^2)/|\mathbf{r}|$  is the Oseen tensor. The equations (2.2) are solved numerically using the adaptive fourth order Runge-Kutta method.

Initially, the particles are placed at vertexes of  $K$  horizontal regular polygons (called 'rings') which are separated from each other vertically and centered one above (or below) the other. The diameter  $d$  of the top ring is taken as the length unit. The number  $N$  of particles in every ring is the same. Therefore, the total number of particles in the system is equal to  $M = KN$ . Because of the system symmetry, we use the cylindrical coordinate system, in which  $\mathbf{r}_i$  is represented as  $\mathbf{r}_i = (\rho_i, \phi_i, z_i)$ .

Searching for periodic solutions, we take into account that numerical non-symmetrical perturbations can destroy periodic unstable solutions after times much smaller than the period, as observed by Ekiel-Jeżewska (2014). Therefore, we symmetrize the dynamics: we force the azimuthal components of the particle velocities to vanish, with  $\phi_i = \text{const}(t)$  for  $i = 1, \dots, M$ . Therefore, the polygons remain regular for all times, and the radial and vertical coordinates of the particles from the same polygon  $k$  are the same,  $\rho_{K(n-1)+k} = \rho_k$  and  $z_{K(n-1)+k} = z_k$  for  $n = 1, \dots, N$  and  $k = 1, \dots, K$ . The system of  $3M$  equations (2.2) is reduced to the system of  $2K$  equations for  $\rho_k$  and  $z_k$ .

We are interested in relative motion of the particles; therefore, we will trace their positions in the centre-of-mass system, located at  $\mathbf{r}_{CM} = (0, 0, z_{CM})$ . In this frame of reference,  $\rho_i$  and  $\phi_i$  are the same, and particle vertical coordinates are  $Z_i = z_i - z_{CM}$ .

We perform simulations for two families of the systems: with two and four rings. The specific initial configurations and their evolution will be discussed in the next sections.

### 3. Dynamics of 2 rings

We first consider a system of  $M = 2N$  particles which are grouped in two horizontal rings, each containing  $N$  equally spaced particles. Initially, the rings are identical and placed one exactly above the other. The diameter of each ring is equal to 1 and the initial distance  $C$  between the rings is a parameter in our simulations, as shown in figure 3(a). The initial positions  $\mathbf{r}_i = (\rho_i, \phi_i, z_i)$  of the particles  $i = 1, \dots, M$  are

$$\mathbf{r}_{2n-1} = \left( \frac{1}{2}, \frac{2\pi n}{N}, \frac{C}{2} \right), \quad \mathbf{r}_{2n} = \left( \frac{1}{2}, \frac{2\pi n}{N}, -\frac{C}{2} \right), \quad n = 1, \dots, N. \quad (3.1)$$

We conducted around 100 simulations for  $M = 256$  and 20000 particles and different

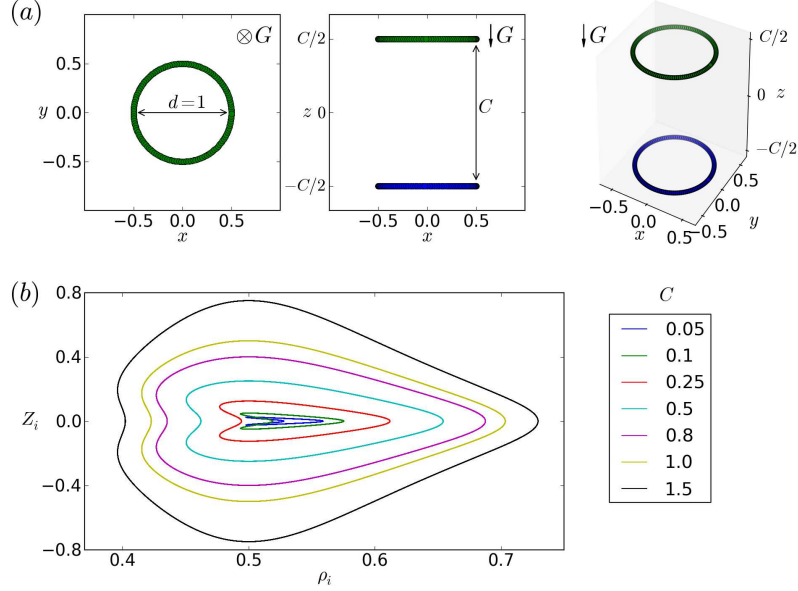


FIGURE 1. The system of  $M$  particles which form 2 rings. (a)  $M = 256$ . The initial configuration as in Eq. (3.1). (b)  $M = 20000$ . In the centre-of-mass frame, the trajectory of each particle has the same shape (not drawn to scale). Different shapes correspond to the indicated values of  $C$ .

initial values of  $C \in [0.05, 2.5]$ . For these values of the parameters, we observe periodic motion of the particles during the whole simulation time  $t = 5000$  (what corresponds to 300-2700 periods), as shown in movie 1.

In the centre-of-mass frame, two particles with the same angular coordinates move along the same trajectory. Its shape is the same for all the pairs, and it depends on  $C$  as shown in figure 1(b) for  $M = 20\,000$ . We found similar families of shapes for  $M = 256$ , analogical to those reported by Ekiel-Jeżewska (2014) for  $M = 16$ , and resembling periodic solutions for rigid rods, discussed by Jung *et al.* (2006) and Bukowicki *et al.* (2015).

## 4. Dynamics of 4 rings

### 4.1. Initial configurations

In the second system,  $M$  particles are grouped in four horizontal rings, each consisting of  $N$  particles. Initially, the rings labeled 1 and 3 are placed at  $z = C/2$  and  $-C/2$ , respectively, and the rings labeled 2 and 4: at  $z = 0$ , as shown in figure 2(a). The radii of the rings 1, 3, 2 and 4 are equal to  $1/2$ ,  $1/2$ ,  $R_2$ , and  $R_4$ , respectively, with  $R_4 > R_2$ . The angular coordinates of the particles from ring 1 and ring 3 are the same. The other rings are rotated by  $\pi/N$  around the symmetry axis. Summarizing, the initial cylindrical coordinates of the particles are,

$$\mathbf{r}_{4n-3} = \left( \frac{1}{2}, \frac{2\pi(n-1)}{N}, \frac{C}{2} \right), \quad \mathbf{r}_{4n-2} = \left( R_2, \frac{2\pi(n-\frac{1}{2})}{N}, 0 \right), \quad (4.1)$$

$$\mathbf{r}_{4n-1} = \left( \frac{1}{2}, \frac{2\pi(n-1)}{N}, -\frac{C}{2} \right), \quad \mathbf{r}_{4n} = \left( R_4, \frac{2\pi(n-\frac{1}{2})}{N}, 0 \right), \quad (4.2)$$

where  $n = 1, \dots, N$  and  $R_2$  and  $R_4$  are the parameters of the simulation.

We performed around 400 000 simulations for clusters made of different numbers of

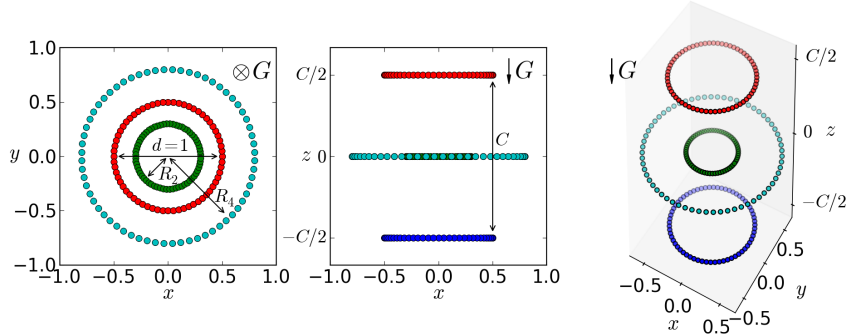


FIGURE 2. Initially,  $M$  particles form 4 rings, as specified in Eq. (4.2). Here,  $M = 256$ .

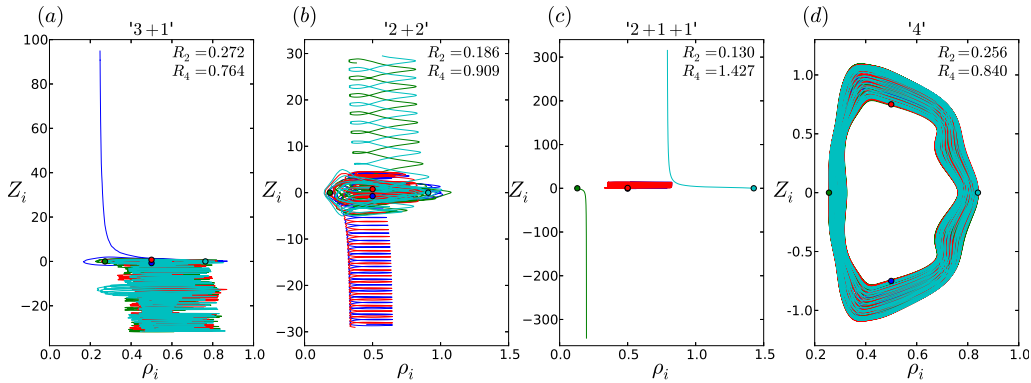


FIGURE 3. Evolution of  $M=256$  particles which form 4 rings. Trajectories of four particles (each from a different ring) in the centre-of-mass reference frame until time  $t=500$ . The initial positions of the particles are marked by dots, with  $C=1.5$  and  $R_2, R_4$  as indicated. (a) ‘3+1’ type of decay. One of the rings separates from the cluster. (b) ‘2+2’ type of decay. The group breaks up into two pairs of oscillating rings - one of them falls faster than the other. (c) ‘2+1+1’ type of decay. The cluster breaks up into one pair of oscillating rings and two single rings. (d) ‘4’: lack of decay. All rings oscillate.

particles  $M=64, 256, 1024$  at the initial configurations specified by Eqs. (4.1)-(4.2), with  $C \in [0.05, 2.5]$ , and a wide range of  $R_2$  and  $R_4$ . In Secs. 4.2-4.4 we will analyze how the dynamics depends on  $R_2$  and  $R_4$  for  $M=256$  and  $C=1.5$ . Then, in Sec. 4.6, we will argue that these results are generic also for the other values of  $M$  and  $C$ .

#### 4.2. Basic features of the dynamics

The dynamics of four rings of particles is more complex than the dynamics of two rings. Although the general pattern of oscillations combined with settling is kept, in case of four rings the motion in general is not periodic and we observe destabilisation and decay of the system, as in movie 2. Majority of initial conditions lead to the system decay during first 1000 units of the simulation time, what corresponds to about 100 oscillations.

If the group breaks up, usually one ring is left behind the other three or one ring falls faster than the rest of the group; we call it ‘3+1’ type of decay. If the system separates into two pairs of rings, we denote it ‘2+2’ type of decay. We observe also ‘2+1+1’ type of decay when two rings oscillate together and the others are separated. Examples of each decay type are presented in figure 3(a)-(c) and movies 3a-c.

For certain initial configurations, the particles perform quasiperiodic motion over a

very long time. It has been checked that for several thousands of values of  $R_2$  and  $R_4$  the cluster lifetime exceeds 100000. A typical shape of the corresponding trajectory  $Z_i(\rho_i)$  is shown in figure 3(d) and movie 3d. These findings may indicate that for certain values of  $R_2$  and  $R_4$ , periodic solutions exist, and they will be searched for later in this paper.

We would like to remind that all simulations are performed for symmetrized configurations and the particles by definition do not change the vertical planes they belong to, as described in Sec. 2. The symmetrisation is done on purpose to find periodic solutions and ensure that the system will not break up because of non symmetrical numerical perturbations before a period is completed.

#### 4.3. Decay of the cluster

To describe the system dynamics, it is crucial to define the event of the cluster decay and its time, denoted as  $\tau$ . The intrinsic property of a cluster of particles settling under gravity is the existence of periodic relative motions which may be used as an indicator whether the particles move together and interact with each other. For this reason we introduce a criterion of a cluster decay based on presence or absence of oscillations between pairs of particles. In particular, oscillations of particles  $i$  and  $j$  which belong to the same group imply that the difference of their  $z$ -coordinates,  $\Delta z_{ij} = z_i - z_j$ , oscillates around zero. We recognise that the particles  $i, j$  interact and stay together if  $\Delta z_{ij}$  has repeating roots.

Therefore, we use the following definition of the cluster decay. For each pair of particles  $i, j$  we calculate the difference  $\Delta z_{ij}$  of their  $z$ -coordinates as a function of time. If for any  $l, m$  the time interval between two consecutive roots,  $t_A$  and  $t_B > t_A$ , of  $\Delta z_{lm}$  exceeds 1000, we classify it as the cluster decay and denote  $\min_{l,m} t_A$  as the cluster lifetime  $\tau$ .

This criterion of decay works well, in contrast to attempts based on measuring only the relative vertical distances between rings, because it is common that rings approach each other again, even though they were separated by a very long vertical distance meanwhile, as observed by Ekiel-Jeżewska & Wajnryb (2011) for systems of three particles.

To define the type of the cluster decay we apply the following procedure: we count the number of roots of  $\Delta z_{ij}$  in the time interval  $[\tau, \min(\tau + 1000, T)]$  for each pair of particles  $ij$ . If the number of roots is smaller than the length of the time interval divided by 200 (for the interval  $[\tau, \tau + 1000]$  it is equal to 5), we define that the particles  $i, j$  interact with each other. Otherwise, we denote them as separated. The number  $L$  of interacting pairs indicates the type of the decay.  $L=3$  corresponds to ‘3+1’ type of the decay,  $L=2$  to ‘2+2’ type of the decay,  $L=1$  to ‘2+1+1’ type of the decay and  $L=0$  to ‘1+1+1+1’. For  $L=6$  there is no decay (type ‘4’).

Now, the main question is how the lifetime depends on initial conditions. The results are presented in figure 4 as a map in space of the parameters  $R_2$  and  $R_4$ , with colours indicating the logarithm of the cluster lifetime. Values of  $(R_2, R_4)$  which lead to long-living clusters form a few compact regions, around which only isolated configurations with long lifetimes can be found. Deterministic regions are visible when  $R_2$  is small enough, or  $R_4$  is large enough, and the cluster splits up immediately without oscillations. In the first case, settling velocity of a very small ring 2 is much larger than velocities of the other rings, while in the second case, settling velocity of a very large ring 4 is much smaller than velocities of the other rings.

The essential property of the map shown in figure 4 is that for a wide range of  $R_2$  and  $R_4$ , the cluster lifetime is very sensitive to initial conditions. Around the regions of long-living clusters (with very sharp edges) we find a variability of the cluster lifetime by orders of magnitude. This property is also well visible in figure 5 at the cross sections of the map, plotted in the linear scale. This behaviour is similar to the chaotic scattering reported by Janosi *et al.* (1997) for three point particles sedimenting in a vertical plane.

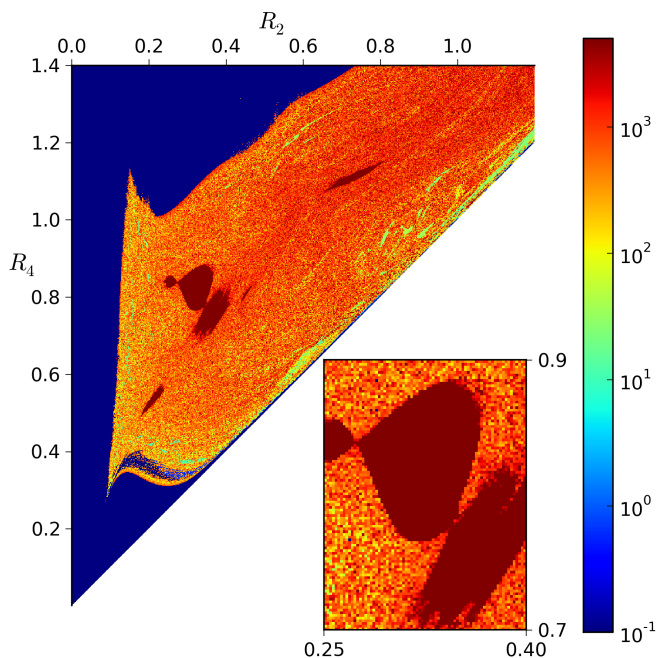


FIGURE 4. The cluster lifetime for around 240 000 initial configurations with  $C = 1.5$  and different values of  $R_2$  and  $R_4$  (drawn to scale). The darkest red colour corresponds to the cluster lifetime larger than the simulation time  $t = 5000$ . Resolution of the map is  $0.002 \times 0.002$  and  $M = 256$ .

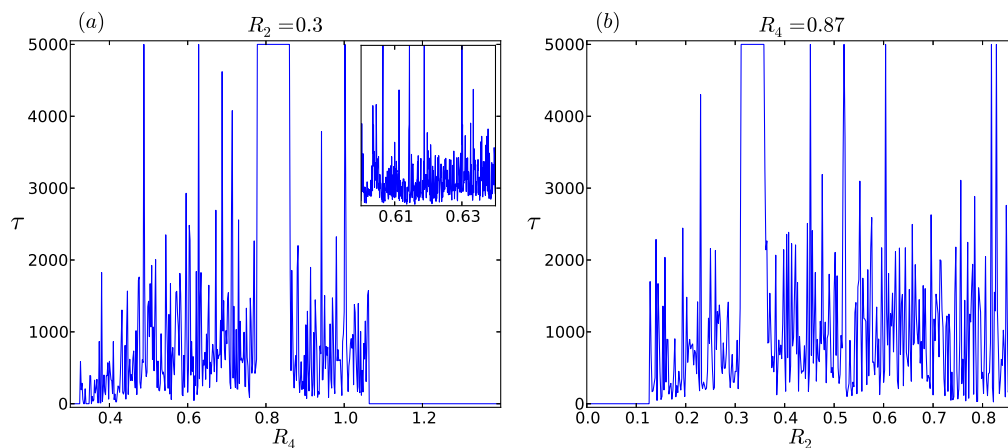


FIGURE 5. Cross-sections (now in the linear scale) through the map of the cluster lifetime from figure 4: (a)  $R_2 = 0.3$ , (b)  $R_4 = 0.87$ . Sensitivity to initial conditions is clearly visible. Inset: Scaling down the resolution of  $R_2$  and  $R_4$  from  $0.002$  to  $10^{-4}$ , a self-similar structure is found.

In figure 6, we show the type of the cluster decay and labels of the particles which interact with each other at the decay time  $\tau$ , depending on  $R_2$  and  $R_4$ . Sensitivity to initial conditions is clearly visible at most of the map areas, except a few deterministic regions corresponding to a very long or very short lifetimes. The last ones can be easily understood by comparing the ring diameters, and taking into account that the smaller the ring, the larger is its velocity.

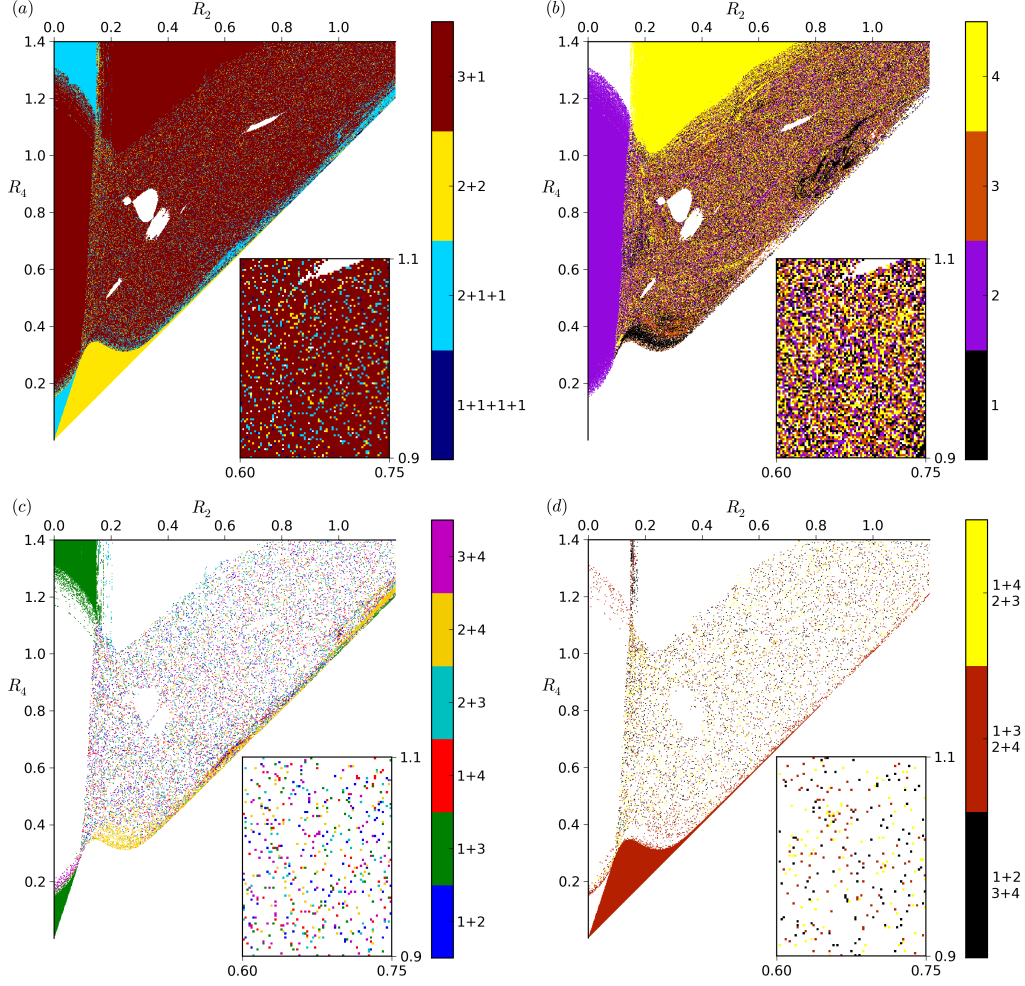


FIGURE 6. Sensitivity of patterns of the cluster decay to the initial parameters  $R_2$  and  $R_4$ , for  $C = 1.5$  and  $M = 256$ . White colour means no decay. (a) The types of the decay: into ‘3+1’, ‘2+2’, ‘2+1+1’ or ‘1+1+1+1’ rings (see Sec. 4.3 for the exact definitions). (b) ‘3+1’ type of the decay: the colour indicates the label of the ring which separates from the others at time  $\tau$ . (c) ‘2+1+1’ type of the decay: the colours indicate the interacting pair of the rings at time  $\tau$ . (d) ‘2+2’ type of the decay: the colours indicate which rings form interacting pairs at time  $\tau$ .

#### 4.4. Clusters with long lifetimes and quasiperiodic solutions

We have found that the long lifespan of the cluster and quasiperiodic trajectories of particles are observed for the system with initial configurations grouped in a few regions (see figure 4). We will now investigate trajectories from each of the specific long-lifetime regions, and search for periodic solutions.

To this goal, we apply the Dynamic Time Warping (DTW) method, described e. g. by Müller (2007) and Vlachos *et al.* (2002). For each particle  $i$ , we define its reference trajectory  $Z_i^r(\rho_i)$  for times  $t_1 \leq t \leq t_3$ , where  $t_k$ ,  $k = 1, 2, 3$ , are the first, second and third time instants when  $Z_i(t_k) = 0$ . Then, for  $t_3 \leq t \leq 5000$ , we calculate the Euclidean distance  $d_i(t)$  between the particle position  $(Z_i(t), \rho_i(t))$  and its reference trajectory. We define

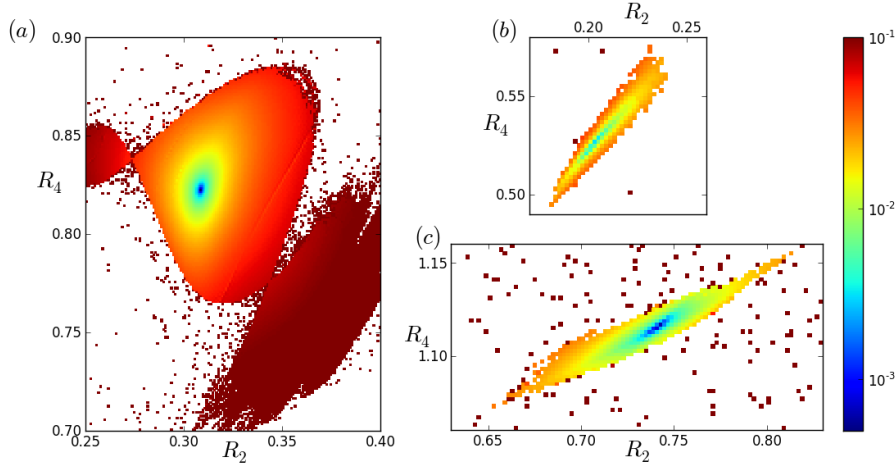


FIGURE 7. The average deviation  $\Delta$  of particle trajectories for clusters with lifetimes  $\tau \geq 5000$ ,  $C=1.5$  and  $M=256$ . Resolution: (a):  $0.001 \times 0.001$ ; (b) and (c):  $0.002 \times 0.002$ .

the average deviation  $\Delta$  of the trajectories as the average of  $d_i(t)$  over all the particles  $i$  and all times  $t$ .

In figure 4, we surround three main long-time islands in the  $R_2$ - $R_4$  space by rectangular boxes of a fixed resolution, and evaluate for each pixel the average deviation  $\Delta$  of the trajectories. The results are shown in figure 7. For each of the three boxes, there exists a smallest deviation  $\Delta_{\min}$ , corresponding to a very thin trajectory. For example, in figure 7(a),  $\Delta_{\min} = 3 \cdot 10^{-4}$  is three hundred times smaller than deviation of the quasiperiodic trajectories shown in figure 3(d).

#### 4.5. Three periodic solutions

The minima visible in figures 7(a),(b),(c) correspond to three periodic trajectories in the centre-of-mass frame of the cluster, shown in figures 8(a),(b),(c), respectively. We remind that owing to the symmetrization of the dynamics, each particle from ring  $i$  has the same coordinates  $Z_i(t)$  and  $\rho_i(t)$ . Therefore, it is sufficient to display  $Z_i(\rho_i)$  for particles  $i=1, 2, 3, 4$ : each from a different ring  $i$ , with particles 1, 3 moving in vertical plane  $\phi=0$  and particles 2, 4 moving in another vertical plane  $\phi=4\pi/M$ . Here,  $M=256$  and  $C=1.5$ .

The new periodic solutions have the following properties.

**Solution 1**, shown in figure 8(a) and movie 8a, is located in the middle of the biggest of the long-lifetime regions from figure 4. All four particles move along the same trajectory  $Z_i(\rho_i)$ , shifted in phase by  $T/4$ , with the period  $T = 11.7$ .

**Solution 2**, shown in figure 8(b) and movie 8b, is located in the middle of a small long-lifetime region from figure 4, with the initial radius  $R_2$  of the ring 2 much smaller than the initial radius of the rings 1 and 3,  $R_1=R_3=0.5$ , and with  $R_4 \gtrsim 0.5$ . The central particle 4 has its own tiny trajectory and is circulated by the other three, which move along a larger trajectory with the period  $T=10.7$ , shifted in phase by  $T/3$  with respect to each other. The period of particle 4 is equal to  $T/3$ .

**Solution 3**, shown in figure 8(c) and movie 8c, is located in the middle of the other small long-lifetime region from figure 4, with  $R_2, R_4 > R_1=R_3=0.5$ . Now particle 2 is the central one, and the motion is qualitatively similar to solution 2, with the interchange of the particles 2 and 4, and much wider rings, what leads to a larger period,  $T = 15.6$ , because larger rings move slower.

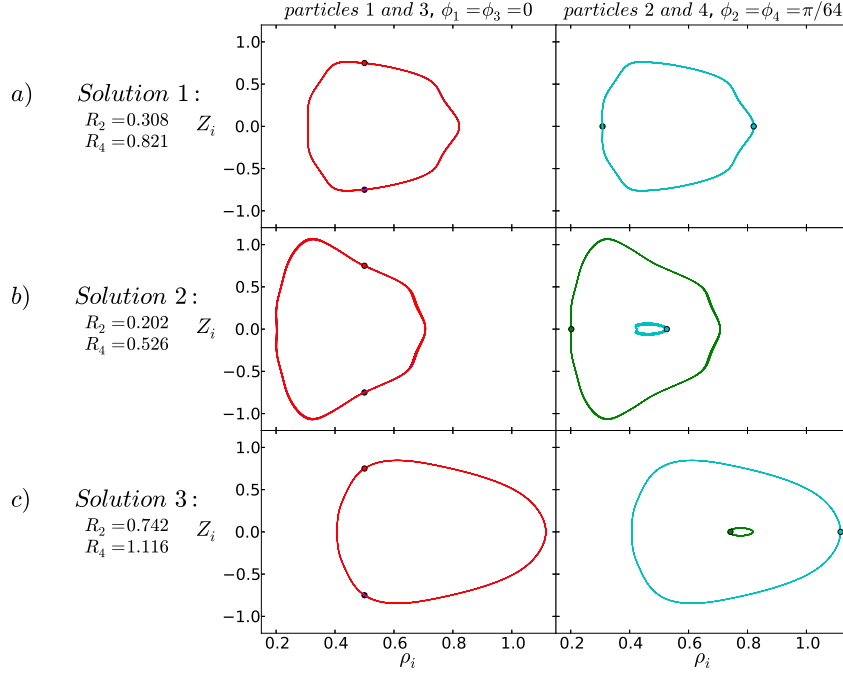


FIGURE 8. Periodic trajectories of four particles (each from a different ring) in the centre of mass frame of a cluster with  $M = 256$  particles. Dots: the initial particle positions, with  $C = 1.5$ .

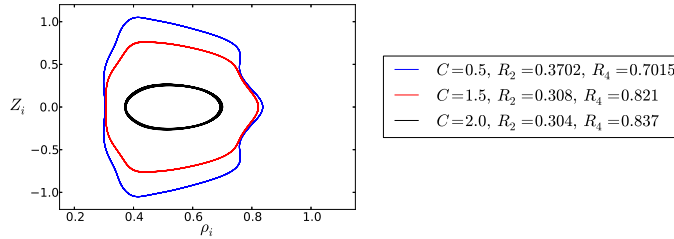


FIGURE 9. Periodic solutions of type 1 for different values of  $C$  and  $M = 256$ .

#### 4.6. Two families of periodic solutions

Periodic oscillations have been found for many values of  $C$ . In figure 9 we show how the shape of the periodic trajectory of type 1 depends on  $C$ . Periodic solutions 1, 2 and 3 for  $C = 2$  are shown in figure 10 in the Supplementary Material. These examples illustrate that the basic properties of the periodic solutions, described in the previous section and shown in figure 8, are generic for a wide range of values of  $C$ .

Initially, two particles are at the same horizontal plane, and the other two particles are exactly one above the other. Movies 8b,c illustrate that for each periodic solution 2 or 3, such a configuration appears again at  $T/6$ , but with *different* values of  $C$ ,  $R_2$  and  $R_4$ , which correspond to solutions 3 or 2, respectively. This new configuration can be treated as another initial condition for the same periodic solution. Therefore, assuming that there exist periodic solutions for all sufficiently large values of  $C$ , we predict the existence of twin solutions 2 and 3 for each value of  $C$  which is large enough.

Dynamics of 4 rings made of other numbers  $M = 64, 1024$  of the particles have been also evaluated, and similar families of periodic solutions have been found.

## 5. Discussion and concluding remarks

In this work, we searched for periodic relative motions of many particles which form regular clusters with aspect ratios of the order of one. We found a surprisingly large number of periodic solutions. For a cluster made of 2 rings, they were observed for all the investigated shapes and particle numbers even as large as 20 000. Clusters made of 4 rings usually break up, and their lifetime and type of decay are in general sensitive to initial conditions. In the 2D space of initial parameters, the deterministic area surrounds the chaotic region which contains islands of quasiperiodic oscillations which do not destabilize during extremely long simulation times. At the centers of these islands, two families of periodic solutions exist, parameterized by the initial cluster height and the number of particles. These findings provide a new perspective for the physical mechanism of hydrodynamic clustering of particles sedimenting in a viscous fluid.

## Acknowledgement

This work was supported in part by the Polish National Science Centre, Grant No. 2011/01/B/ST3/05691. We benefited from scientific activities of the COST Action MP1305.

## REFERENCES

- BUKOWICKI, M., GRUCA, M. & EKIEL-JEŻEWSKA, M. L. 2015 Dynamics of elastic dumbbells sedimenting in a viscous fluid: oscillations and hydrodynamic repulsion *J. Fluid Mech.* [in print]
- CAFLISCH, R. E., LIM, C., LUKE, J. H. C. & SANGANI, A. S. 1988 Periodic solutions for three sedimenting spheres. *Phys. Fluids* **31**, 3175.
- EKIEL-JEŻEWSKA, M. L., GUBIEC, T., SZYMCAK, P. 2008 Stokesian dynamics of close particles, *Phys. Fluids* **20**, 63102.
- EKIEL-JEŻEWSKA, M. L. 2008 Periodic orbits of Stokesian dynamics. *CDROM Proceedings of the XXII International Congress of Theoretical and Applied Mechanics*, edited by J. Denier, M. D. Find and T. Mattner. University of Adelaide; ISBN: 978-0-9805142-1-6.
- EKIEL-JEŻEWSKA, M. L., WAJNRYB, E., 2011 Lifetime of a cluster of spheres settling under gravity in Stokes flow, *Phys. Rev. E*, **83**, 067301.
- EKIEL-JEŻEWSKA, M. L. 2014 Class of periodic and quasiperiodic trajectories of particles settling under gravity in a viscous fluid, *Phys. Rev. E*, **90**, 043007.
- HOCKING, L. M. 1963 The behaviour of clusters of spheres falling in a viscous fluid. *J. Fluid Mech.* **20**, 129–139.
- JAYAWEERA, K. O. L. F., MASON, B. J. & SLACK, H. W. 1964 The behaviour of clusters of spheres falling in a viscous fluid. Part 1. Experiment. *J. Fluid Mech.* **20**, 121–128.
- JANOSI, I. M., TEL, T., WOLF, D. E. & GALLAS, J. A. C. 1997 Chaotic particle dynamics in viscous flows: The three-particle Stokeslet problem. *Phys. Rev. E* **56**, 2858–2868.
- JUNG, S., SPAGNOLIE, S. E., PRIKH, K., SHELLEY, M. & TORNBORG, A. K. 2006 Periodic sedimentation in a Stokesian fluid. *Phys. Rev. E* **74**, 035302(R).
- KIM, S. & KARRILA, S. J. 2005 *Microhydrodynamics. Principles and Selected Applications*. Dover Publications, Inc., New York.
- MÜLLER, M. 2007 *Information Retrieval for Music and Motion*. Springer-Verlag, Berlin Heidelberg.
- MYŁYK, A., MEILE, W., BRENN, G. & EKIEL-JEŻEWSKA, M. L. 2011 Break-up of suspension drops settling under gravity in a viscous fluid close to a vertical wall *Phys. Fluids*. **23**, 063302.
- TORY, E. M., KAMEL, M. T. & TORY, C. B. 1991 Sedimentation of clusters of identical spheres. III. Periodic motion of four spheres. *Powder Technology* **67**, 71–82.
- VLACHOS, M., KOLLIOS, G. & GUNOPULOS, D. 2002 Discovering Similar Multidimensional Trajectories *Proceedings of the 18th International Conference on Data Engineering*, 673–684.